PRL, 2006

Swinging of red blood cells under shear flow

Manouk Abkarian[1,3],* Magalie Faivre[2,3], and Annie Viallat[2,3†]
1. Laboratoire des Colloïdes, Verres et Nanomatériaux,
UMR 5587, CNRS/UM2, CC26, 34095 Montpellier Cedex 5, France
2. Laboratoire Adhésion et inflammation, Inserm U600/CNRS UMR 6212 Université de la Méditerranée,
Case 937, 163 Av. de Luminy, 13288 Marseille Cedex 9, France
3. Laboratoire de Spectrométrie Physique, UMR 5588 CNRS/UJF, BP 87, 38402 Saint Martin d'Hères, France
(Dated: January 16, 2007)

We reveal that under moderate shear stress ($\eta\dot{\gamma} \approx 0.1$ Pa) red blood cells present an oscillation of their inclination (swinging) superimposed to the long-observed steady tanktreading (TT) motion. A model based on a fluid ellipsoid surrounded by a visco-elastic membrane initially unstrained (shape memory) predicts all observed features of the motion: an increase of both swinging amplitude and period (1/2 the TT period) upon decreasing $\eta\dot{\gamma}$, a $\eta\dot{\gamma}$-triggered transition towards a narrow $\eta\dot{\gamma}$-range intermittent regime of successive swinging and tumbling, and a pure tumbling motion at lower $\eta\dot{\gamma}$-values.

PACS numbers: 83.50-v; 83.80.Lz; 87.17.Jj
Keywords: tank treading; tumbling; capsule; membrane elasticity; shape memory

A human red blood cell (RBC) is a biconcave flattened disk, essentially made of a Newtonian hemoglobin solution encapsulated by a fluid and incompressible lipid bilayer, underlined by a thin elastic cytoskeleton (spectrin network) [1]. The complex structure of RBCs and their response to a viscous shear flow have a great influence on flow and mass transport in the microcirculation in both health and disease [2]. The full understanding of this response requires a direct comprehensive observation of cell motion and deformation, and a model for deducing the cell intrinsic properties from its behavior in shear flow. It is generally admitted that the two possible RBC movements are the unsteady tumbling solid-like motion [3], and the drop-like 'tanktreading' motion for higher shear stresses, where the cell maintains a steady orientation, while the membrane rotates about the internal fluid, as reported respectively for RBCs suspended in plasma or in high-viscosity media and submitted to high shear stresses [3, 4, 5, 6]. However, the RBC movement at smaller shear rate and close to the tumbling-tanktreading transition, has not been fully explored. Moreover, the actual state of deformation of the elastic skeleton either in the flowing or in the resting RBC is still conjectural ("shape memory" problem) [7]. Most models [6, 8] derive from the analytical framework of Keller and Skalak (KS) [9], which treats the RBC as a fluid ellipsoidal membrane enclosing a viscous liquid. Although this model qualitatively retrieves the two modes of motion, it does not capture the observed shear-rate dependency of the tumbling-tanktreading transition. In particular, the model does not account for the possible elastic energy storage induced by the local deformations of the cytoskeleton during tanktreading. Approaches including membrane elasticity are either restricted to spherical resting shapes because of analytical complexities [10], or propose encouraging but still limited numerical analysis on tanktreading elastic biconcave capsules [11].

Here, we reveal a new regime of motion for RBCs under small shear flow, characterized by an elastic capsule-like oscillation of the cell inclination superimposed to tanktreading that we name swinging. We develop a model, which predicts both swinging and the shear-stress dependency of the tumbling-tanktreading transition. It demonstrates the existence of the elastic shape memory in the membrane.

Direct measurements of cell orientation with respect to the flow direction (angle θ) and cell shape (lengths of the long and small axis of the cell cross-section, a_1 and a_2 respectively) are provided from side-view microscopic imaging in a vertical plane parallel to the plane of shear [12]. We varied the wall shear rate $\dot{\gamma}$ (in the range 0-5 s^{-1}) and the outer viscosity η_o by suspending RBCs in various solutions of dextran (concentration 6%, 7.5% or 9% w/w and viscosity 22, 31 and 47 mPa.s respectively). Therefore, the wall shear stress is varied in a range from 0 to 0.25 Pa. For the highest values of the external shear stress $\eta_o\dot{\gamma}$, tanktreading is observed. It is characterized by i) a quasi-stationary cell shape with insignificant deformation (maximum variation of $a_1 \leq 5\%$), ii) rotation of the membrane, revealed from the motion of small carboxylated beads stuck to the membrane (Fig. 1B) and iii) an oscillation of the cell inclination about a mean value ranging from 6° to 25° (Figs. 1C and 2, see [13]) at a frequency equal to twice the tanktreading frequency (Fig. 1B). Such characteristics are not seen on tanktreading viscous lipid vesicles [12, 14], neither predicted [9, 15, 16, 17]. This oscillation is however observed for non-perfectly spherical elastic millimeter-scale capsules [18, 19] (Fig. 2B) or protein-coated drops [20], and in numerical simulations on biconcave elastic shells [11]. We explain this phenomenon by assuming RBC shape memory. We state that the local elements of the composite membrane (cytoskeleton and lipid bilayer), including the elements which form the rim and the dim-

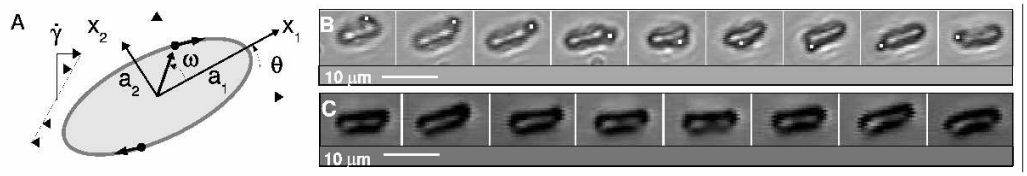

FIG. 1: Units $[\eta_i]=[\eta_o]=[\eta_m]$=mPa.s, $[\mu]$=Pa and .$[\dot{\gamma}]$=s^{-1}. (A) Schematic drawing of a tanktreading ellipsoid in a shear flow. (B) Rotation of a bead (diameter 1μm) stuck on the membrane of a RBC with ($\dot{\gamma}$ = 6, η_o = 47). Time sequence of 1s. (C) RBC swinging : ($\dot{\gamma}$ = 1.33, η_o = 47). Time sequence of 2s.

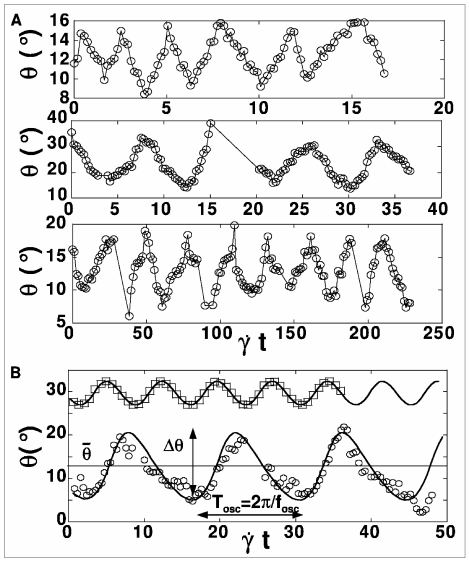

FIG. 2: Same units as in Figure 1. (A) Orientation versus the normalized time $\dot{\gamma}$t for various cells from top to bottom: ($\dot{\gamma}$ = 1.8, η_o = 22), ($\dot{\gamma}$ = 2.6, η_o = 31), ($\dot{\gamma}$ = 6.6, η_o = 47). (B) Orientation versus $\dot{\gamma}$t for: (○) a RBC with ($\dot{\gamma}$ = 0.8, η_o = 47); solid line from (Eq. 2) with (η_m = 1120, μ_m = 0.42); (□) a polymeric capsule from [19] with ($\dot{\gamma}$ = 18, η_o = 964). Solid line from (Eqns. 2) with the surface moduli ($\eta_m.e$ = 0.085 mPa.s/m, $\mu_m.e$ = 0.675 mPa.m), and (a_1 = 278.8μm, a_2 = a_3 = 170.8 μm) obtained from the size at rest R_0 = 224.8 μm of the capsule and its mean deformation during flow: $D = (a_1 - a_2)/(a_1 + a_2) \approx 0.12$ at $\dot{\gamma}$ = 18.

ples are not equivalent and are not strained in the biconcave resting shape. They do consequently not store elastic energy. Thus, during tanktreading, the elements which form the rim at rest rotate about the stationary cell shape to reach the dimples after rotation and reciprocally. These elements are then locally strained and store elastic energy. Both local deformation and energy storage are periodic: each time the elements of the membrane make a π-rotation, they retrieve their initial shape and are no more strained. We emphasize that the periodic storage of energy requires a non spherical unstrained state for the RBC. Otherwise, the membrane elements will tanktread without modifying the global state of stress of the cell, preserving the steady nature of the tanktreading movement.

In order to derive tractable equations of motion, we use the KS model. We consider an oblate ellipsoid filled with a viscous liquid and delimited by a viscoelastic 3D thin membrane, which includes the lipid bilayer and the underlying cytoskeleton [21]. The membrane elements are prescribed to rotate along elliptical trajectories parallel to the shear plane, with a linear velocity field [22] given by: $v_1 = -\dot{\omega}(a_1/a_2)x_2, v_2 = \dot{\omega}(a_2/a_1)x_1, v_3 = 0$, where ω and $\dot{\omega}$ are the phase angle of a membrane element and its instantaneous frequency of tanktreading respectively (Fig. 1A). The KS equation for RBC motion is obtained by stating that at equilibrium, the total moment exerted by the external fluid on the cell vanishes (First equation in Eqs.2 below). In addition, the movement satisfies the conservation of energy, i.e. the rate of dissipation of energy in the cell must equal the rate at which work is done by the external fluid on the cell. KS calculated both rates assuming viscous energy dissipation in the cell. We add to this latter contribution the elastic power stored in the periodic elastic strain of the cytoskeleton [24]: $P_{el} = \int_\Omega \mathrm{Tr}(\sigma : \mathbf{D})\mathrm{d}\Omega$, where Ω is the membrane volume, $\mathbf{D}$ the eulerian strain rate tensor derived from the KS velocity field and σ the shear stress tensor in the membrane; σ is computed from the local deformation of the membrane due to tanktreading, assuming a simple Kelvin-Voigt viscoelastic material: $\sigma = 2\eta_m\mathbf{D} + 2\mu_m\mathbf{E}$, where $\mathbf{E}$ is the Euler-Almansi strain tensor obtained from the KS velocity field. After some algebra, P_{el} writes as

$$P_{el} = \frac{1}{2}\dot{\omega}(\frac{a_2}{a_1} - \frac{a_1}{a_2})^2[2\eta_m\dot{\omega} + \mu_m sin(2\omega)]\Omega \qquad (1)$$

where η_m and μ_m are the membrane viscosity and the shear modulus respectively. Conservation of energy provides a constraint on the allowable RBC motion and yields a second differential equation (for more details see [13]). The two coupled equations are:

$$\begin{aligned}\dot{\theta} &= -(\frac{1}{2}\dot{\gamma} + \frac{2a_1a_2}{a_1^2+a_2^2}\dot{\omega}) + \frac{1}{2}\dot{\gamma}\frac{a_1^2-a_2^2}{a_1^2+a_2^2}cos(2\theta)\\ \dot{\omega} &= -\frac{\eta_o f_3\dot{\gamma}}{\eta_o f_2 - \eta_i(1+\frac{\eta_m}{\eta_i}\frac{\Omega}{V})f_1}cos(2\theta)\\ &\quad + \frac{\frac{1}{2}f_1\mu_m\frac{\Omega}{V}}{\eta_o f_2 - \eta_i(1+\frac{\eta_m}{\eta_i}\frac{\Omega}{V})f_1}sin(2\omega)\end{aligned} \qquad (2)$$

where $\dot{\theta}$ is the time derivative of the cell inclination,

f_1, f_2 and f_3 are geometrical constants and V is the RBC volume (same definition as in [9]). The limiting case $\mu_m = \eta_m = 0$ corresponds to KS. We numerically solved the equations using the following set of parameters for RBCs : $a_1 = a_3 = 4\mu$m, $a_2 = 1.5\mu$m, $\Omega = \Sigma.e$ [25], where Σ is the oblate ellipsoid area and e=50 nm is the membrane thickness [26]. η_i is fixed at the physiological value of 10 mPa.s [6] and η_m is adjusted in the range 0.7-2 Pa.s [6]. We obtain $\theta(t)$, $\dot{\theta}(t)$, $\omega(t)$ and $\dot{\omega}(t)$. Suitable couples of μ_m and η_m values were found to reproduce experimental RBC oscillations as seen in Fig. 2B (see [13]). One example of experimental capsule oscillation extracted from [19] is presented as well in Fig. 2B. An insight of experimental and numerical swinging curves is provided from three parameters: the magnitude $\Delta\theta = \theta_{max} - \theta_{min}$, the mean angle $\bar{\theta}$ and the period T_{osc} (or the frequency f_{osc}) of oscillation (Fig. 2B). The $\dot{\gamma}$-variations of these parameters are illustrated for one red blood cell in Fig. 3A together with a numerical solution of Eqns 2. While $\bar{\theta}$ decreases for decreasing $\dot{\gamma}$ down to 0, T_{osc} and $\Delta\theta$ increase until $\dot{\gamma}$ reaches a critical value $\dot{\gamma}_c^-$ below which the cell tumbles at least once. Besides direct observations (Fig. 1B), we illustrate the factor 2 of proportionality between f_{osc} and $\dot{\omega}$ which relates the movement of swinging of a cell to the movement of tanktreading of its membrane, by reporting on a same graph in Fig. 3B, variations of $f_{osc}/2$ and $\dot{\omega}$ versus $\dot{\gamma}$, for different swinging RBCs observed in our experiment and for different tanktreading RBCs observed in the litterature at higher $\dot{\gamma}$ [5, 6]. Fig. 3B shows indeed the continuity of the two regimes even though measured on different type of movement. Therefore, all experimental characteristics are well captured by the model. Indeed, by treating the elastic contribution as a small perturbation in the second equation of (2), valid in the linear part, one recovers the steady KS solution at the order 0 of the parameter in front of $sin(2\omega)$, while at the first order one finds that θ oscillates at twice the tanktreading frequency (linear in $\dot{\gamma}$) and $\Delta\theta$ scales as $(\mu_m/\dot{\gamma})$.

Contrarily to KS prediction, we observe that the transition of movement from tumbling to tanktreading (respectively tanktreading to tumbling) is induced by tuning up (respectively down) the applied shear rate. This transition is illustrated in Fig. 4A. Its more striking feature, predicted and experimentally observed is the existence of a regime of movement where the cells present successively swings and tumbles at a given $\dot{\gamma}$ (Fig. 4B). The model gives the $\dot{\gamma}$-range ($[\dot{\gamma}_c^+, \dot{\gamma}_c^-]$) where this regime exists. Given the experimental constraints, it is not easy to follow the cells sufficiently long to observe a large series of tumbles and swings. We define over a time scale of ~ 20 s, the shear rate corresponding to a change in movement from swinging to tumbling ($\dot{\gamma}_c^<$) with decreasing $\dot{\gamma}$, and from tumbling to swinging ($\dot{\gamma}_c^>$) with increasing $\dot{\gamma}$. The difference $\dot{\gamma}_c^>$ - $\dot{\gamma}_c^<$, that we call hysteresis (for instance for two different RBCs at η_o =31 mPa.s : $\dot{\gamma}_c^< = 0.47$ s^{-1} , $\dot{\gamma}_c^> = 1$ s^{-1} and $\dot{\gamma}_c^< = 0.8$ s^{-1}, $\dot{\gamma}_c^> = 1.73$ s^{-1} respectively) has the same order of magnitude than the theoretical $\dot{\gamma}$-range $[\dot{\gamma}_c^+, \dot{\gamma}_c^-]$ of intermittency. Finally as it is seen by requiring the second term in the second equation of (2) to be of the same order of magnitude as the first part, the critical shear rate should scale as μ_m/η_o. It is indeed numerically observed (Fig. 4C). Both critical values of $\eta_o\dot{\gamma}_c^+$ and $\eta_o\dot{\gamma}_c^-$ are mainly governed by the RBC elastic contribution for given cell geometry and may provide an average determination of μ_m by observing a

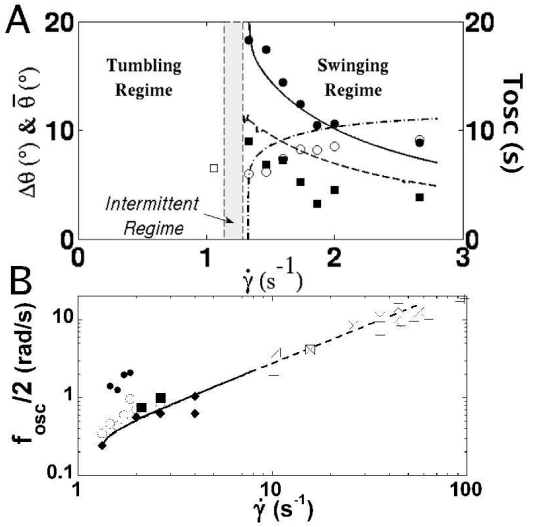

FIG. 3: Same units as in Fig. 1. (A) Experimental data on a single RBC at $\eta_o = 22$: (•) $\Delta\theta$, (■) T_{osc}, (□) 1 tumbling period value and (○) $\bar{\theta}$ versus $\dot{\gamma}$. Corresponding curves of the model with $\mu_m = 0.38$ and $\eta_m = 700$: (—) $\Delta\theta$, (- - -) T_{osc} and $(- \cdot -)$ $\bar{\theta}$. (B) $f_{osc}/2$ versus $\dot{\gamma}$: (•) $\eta_o = 22$; (♦) $\eta_o = 47$; (■) $\eta_o = 31$; (○) Single RBC, $\eta_o = 22$. (×) Tanktreading frequencies $\dot{\omega}$ taken from [6] with $\eta_o = 35$, (+) from [5] with $\eta_o = 18$, 31, and 59, (⊠) from [4] with $\eta_o = 70$. The line is a guide for the eyes.

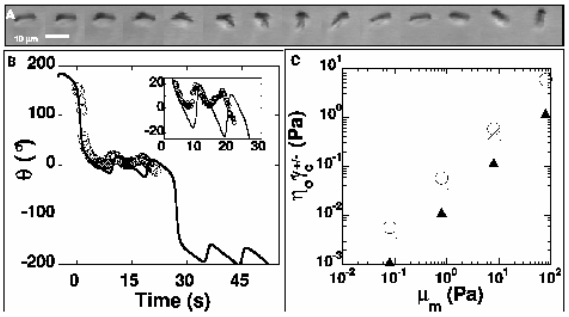

FIG. 4: Same units as in Fig. 1. (A) The transition from swinging to tumbling induced by decreasing $\dot{\gamma}$ is associated with a transient localized deformation (η_o=47, $\dot{\gamma}$=2.66). Time sequence of 1s. (B) (○) Successive swinging and tumbling at ($\eta_o = 22$, $\dot{\gamma}$=1.526); $(---)$ numerical calculus with ($\eta_o = 22$, $\dot{\gamma}$=1.526, $\mu_m = 0.454$, $\eta_m = 700$). (C) Theoretical shear-stresses of transition versus μ_m with $\eta_m = 1000$: (○) $\eta_o\dot{\gamma}_c^-$; (×) $\eta_o\dot{\gamma}_c^+$ and (▲) $\eta_o(\dot{\gamma}_c{}^- - \dot{\gamma}_c{}^+)$.

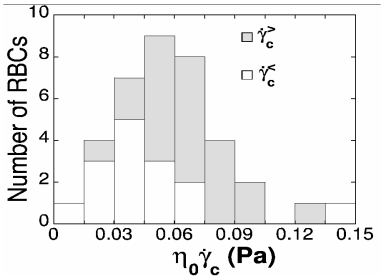

FIG. 5: Distribution function of critical shear stresses of transition for increasing ($\dot{\gamma}^>$) and decreasing ($\dot{\gamma}^<$) shear rates.

large sample of RBCs (Fig. 4C). Distribution functions of $\eta_o\dot{\gamma}_c^>$ and $\eta_o\dot{\gamma}_c^<$ measured on a large RBC sampling are shown in Fig. 5. They characterize the natural variability of the RBC elastic modulus and illustrates the additional hysteresis effect. From Fig. 5 and Fig. 4C, we find that μ_m ranges in the interval 0.14-2 Pa. By setting the 2D shear modulus $\mu_{m,S} = \mu_m.e$ we obtain values ranging from 0.07 to 1×10^{-7} N/m (e = 50 nm) below that usually reported [1, 10]. We also find a comparable difference on $\mu_{m,S}$ with that reported for the elastic capsules by Walter et al [19]. This underestimation likely originates from the major simplifications we made in order to obtain simple analytical equations allowing the full understanding of the physics of the problem: i) simplistic constitutive equations, ii) approximate KS velocity field, which may overestimate membrane deformations. In particular, Tran son Tay et al [6] suggested that the Secomb-Skalak area conserving velocity field [23] would lead to a 70%-increase of the membrane viscosity compared to that derived from the KS model. iii) treatment of deformations from a 3D description of the membrane of RBCs and capsules although these systems form mainly 2D-shells [21]. However, the main interest of this tractable model is to understand the role of the various physical parameters on the movement. For example, for given external viscosity and shear rate, $\Delta\theta$ is not much sensitive to values of η_i and η_m taken in the physiological range. $\Delta\theta$ is essentially fixed by μ_m, and thus the measurement of the amplitude of swinging as a function of the shear stress may provide a complementary method to accurately determine μ_m on single flowing RBCs in a given sample.

In conclusion, the swinging movement and the shear-stress triggered transition of motion of RBCs demonstrate the existence of their shape memory and is a signature of their membrane shear elasticity. Despite its simplicity, our model provides a good description of the observed behaviors and we believe that a more sophisticated model should allow an easy and sensitive determination of individual RBC mechanical properties. Finally, such experimental approach coupled to the refined model might be applied to a wide variety of soft shells [18, 19, 20] and holds promises for applications in surface rheology measurements.

We would like to thank Dr. J. Skotheim for discussions, B. Carpentier for experimental help, Pr. H. A. Stone for fruitful discussions and Pr. H. Rehage for providing us with the data on the capsule used in Fig. 2B.

* Electronic address: abkarian@lcvn.univ-montp2.fr
† Electronic address: viallat@marseille.inserm.fr

[1] N. Mohandas and E. Evans, Annu. Rev. Biophys. Biomol. Struct. **23**, 787 (1994).
[2] S. Chien, Ann. Rev. Physiol. **49**, 177 (1987).
[3] H. Goldsmith and J. Marlow, Proc. R. Soc. Lond. B. **182**, 351 (1972).
[4] T. Fischer and H. Schmid-Schnbein, Blood Cells **3**, 351 (1977).
[5] T. Fischer, M. Stöhr-Liesen, and H. Schmid-Schönbein, Science **202**, 894 (1978).
[6] R. Tran-Son-Tay, S. Sutera, and P. Rao, Biophys. J. **46**, 65 (1984).
[7] T. Fischer, Biophys. J. **86**, 3304 (2004).
[8] S. Sutera, P. Pierre, and G. Zahalak, Biorheology **26**, 177 (1989).
[9] S. Keller and R. Skalak, J. Fluid Mech. **120**, 27 (1982).
[10] D. Barthes-Biesel and J. Rallison, J. Fluid. Mech. **113**, 251 (1981).
[11] S. Ramanujan and C. Pozrikidis, J. Fluid Mech. **113**, 251 (2005).
[12] M. Abkarian and A. Viallat, Biophys. J. **89**, 1055 (2005).
[13] movies EPAPS#: sequence of RBC swinging and #: Numerical sequence of tumbling-swinging transition.#: Supplementary information to deduce the Eqns 2.
[14] V. Kantsler, and V. Steinberg, Phys. Rev. Lett. **96**, 6001 (2006).
[15] M. Kraus, W. Wintz, U. Seifert, and R. Lipowsky, Phys. Rev. Lett. **77**, 3685 (1996).
[16] H. Noguchi, and G. Gompper, Phys. Rev. Lett. **93**, 8102 (2004)
[17] C. Misbah, Phys. Rev. Lett. **96** 8104 (2006),
[18] K. Chang and W. Olbricht, J. Fluid Mech. **250**, 609 (1993).
[19] A. Walter, H. Rehage, and H. Leonhard, Colloids Surf. A **183**, 123 (2001).
[20] P. Emi, P. Fischer, and E. Windhab, Appl. Phys. Lett. **87**, 24:4104 (2005).
[21] Because of the 3D nature of the KS velocity field, the membrane deformation is considered to be 3D while other non algebraically tractable approaches considered the deformation field to be only 2D [6, 23].
[22] The KS velocity field is not area conserving. However improved models [23] that account for incompressibility are much more complex algebraically and it is generally considered that the simple KS velocity field provides a good approximation of the membrane deformation [6].
[23] T.W. Secomb, and R. Skalak, Q. J. Mech. Appl. Math. XXXV **2**, 233 (1982).
[24] J.M. Skotheim, and T.W. Secomb, submitted (2006).
[25] Surface area of an oblate ellipsoid: $\Sigma = 2\pi {a_1}^2[1 + (a_2/a_1)^2 \mathrm{atanh}(ex)/ex]$ with $ex = (1 - a_2^2/a_1^2)^{1/2}$.
[26] V. Heinrich, K. Ritchie, N. Mohandas, E. Evans, Biophys. J. **81**, 1452 (2001)